BMB Reports - Manuscript Submission

Manuscript Draft

**Manuscript Number**: BMB-21-018

**Title**: MUC1-C influences cell survival in lung adenocarcinoma Calu-3 cells after SARS-CoV-2 infection

**Article Type**: Article

**Keywords**: Calu-3; lung epithelial cancer; Mucin 1; SARS-CoV-2; STAT3

**Corresponding Author**: Hyung-Joo Kwon

**Authors**: Dongbum Kim[1,#], Sony Maharjan[1,#], Jinsoo Kim[2,#], Sangkyu Park[3], Jeong-A Park[3], Byoung Kwon Park[1], Younghee Lee[3], Hyung-Joo Kwon[1,2,*]

**Institution**: [1]Institute of Medical Science and [2]Department of Microbiology, College of Medicine, Hallym University,
[3]Department of Biochemistry, College of Natural Sciences, Chungbuk National University,

**Manuscript Type:** Article

# MUC1-C influences cell survival in lung adenocarcinoma Calu-3 cells after SARS-CoV-2 infection

Dongbum Kim[1,#], Sony Maharjan[1,#], Jinsoo Kim[2,#], Sangkyu Park[3], Jeong-A Park[3], Byoung Kwon Park[1], Younghee Lee[3,*], Hyung-Joo Kwon[1,2,*]

[1]Institute of Medical Science, College of Medicine, Hallym University, Chuncheon 24252, Republic of Korea

[2]Department of Microbiology, College of Medicine, Hallym University, Chuncheon 24252, Republic of Korea

[3]Department of Biochemistry, College of Natural Sciences, Chungbuk National University, Cheongju 28644, Republic of Korea

**Running Title:** MUC1-C expression after SARS-CoV-2 infection

**Keywords:** Calu-3, lung epithelial cancer, Mucin 1, SARS-CoV-2, STAT3.

**Correspondence to:** Younghee Lee, Tel: +82-43-261-3387; Fax: +82-43-267-2306; E-mail: yhl4177@cbnu.ac.kr; Hyung-Joo Kwon, Tel: +82-33-248-2635; Fax: +82-33-241-3640; E-mail: hjookwon@hallym.ac.kr

[#]These authors have contributed equally to this work

**ABSTRACT**

Severe acute respiratory syndrome coronavirus 2 (SARS-CoV-2) induces coronavirus disease 2019 (COVID-19) and may increase the risk of adverse outcomes in lung cancer patients. In this study, we investigated the expression and function of mucin 1 (MUC1) after SARS-CoV-2 infection in the lung epithelial cancer cell line Calu-3. MUC1 is a major constituent of the mucus layer in the respiratory tract and contributes to pathogen defense. SARS-CoV-2 infection induced MUC1 C-terminal subunit (MUC1-C) expression in a STAT3 activation-dependent manner. Inhibition of MUC1-C signaling increased apoptosis-related protein levels and reduced proliferation-related protein levels; however, SARS-CoV-2 replication was not affected. Together, these results suggest that increased MUC1-C expression in response to SARS-CoV-2 infection may trigger the growth of lung cancer cells, and COVID-19 may be a risk factor for lung cancer patients.

## INTRODUCTION

Severe acute respiratory syndrome coronavirus 2 (SARS-CoV-2) is a lineage B betacoronavirus that is responsible for the current coronavirus disease 2019 (COVID-19) pandemic. COVID-19 first appeared in Wuhan City, China in December 2019 (1, 2). By March 17, 2021, the World Health Organization reported that SARS-CoV-2 had infected 120,383,919 people and resulted in the death of 2,664,386 individuals since January 2020 (https://covid19.who.int).

Clinical reports suggest that age, gender, and comorbidities are risk factors for morbidity, complications, and mortality of COVID-19 patients (3). Adults ≥65 years old show more severe illness and higher mortality rates (3). Comorbidities that increase the risk of COVID-19 include diabetes, obesity, chronic kidney disease, solid organ transplant, and cancer. Indeed, a recent report from Wuhan University demonstrated that cancer patients were hospitalized at a two-fold higher rate than the general population (4, 5). Given the clinical complexity of cancer, it is critical to develop management plans for cancer patients that contract COVID-19 (6). As lung cancer is the leading cause of cancer death worldwide (7) and SARS-CoV-2 infects the respiratory track, COVID-19 is a key concern for lung cancer patients (8, 9).

Mucins are high molecular weight glycoproteins that are prominently expressed in respiratory, gastrointestinal, and reproductive tracts. The human mucin (MUC) family primarily consists of secreted and transmembrane mucins, which function as physical barriers to pathogens (10). MUC1, a type I transmembrane mucin, is expressed as a single protein that is auto-cleaved at the SEA (sea-urchin sperm protein, enterokinase and agrin) domain to form two heterodimerizing subunits: MUC1-N and MUC1-C (11, 12). Whereas MUC1 expression is localized to the apical surface of normal epithelia, MUC1 is overexpressed in the entire membrane of malignant tumors, such as breast, pancreatic, colon, and lung. Furthermore,

MUC1-C is a well-known oncoprotein that is involved in various signaling pathways, including signal transducer and activator of transcription 3 (STAT3), glycogen synthase kinase 3 beta (GSK-3β), and β-catenin, which are implicated in the maintenance of cancer cells (13-16). MUC1, along with the secretory mucin, MUC5AC, is overexpressed in non-small cell lung cancer and seems to be closely associated with cancer progression (17, 18). Based on these observations, MUC1 has been studied as a potential therapeutic target in many cancers, including lung cancer (17-19).

Here, we investigated MUC1-C expression and function after SARS-CoV-2 infection in the human airway epithelial cell line Calu-3 as a model for lung cancer cells. We confirmed involvement of STAT3 in SARS-CoV-2-induced MUC1-C expression and investigated the effect of MUC1-C inhibition on viral replication and cell viability.

## RESULTS

### SARS-CoV-2 infection induces MUC1-C expression in Calu-3 cells

Many COVID-19 patients have difficulty breathing partially due to excessive mucus formation (20). As MUC1 is a major constituent of the mucus layer in the respiratory system, we investigated the impact of SARS-CoV-2 infection on MUC1 expression in Calu-3 cells using an antibody that recognizes the intracellular C-terminal region of MUC1. As controls, Calu-3 cells were cultured without infection (mock infection). We found that MUC1-C expression was slightly elevated during culture in mock-infected cells and was markedly induced by SARS-CoV-2 (Fig. 1A). Specifically, we observed that SARS-CoV-2 infection promptly induced MUC1-C expression at 12 h. Moreover, SARS-CoV-2-induced MUC1-C expression continued to rise up to 24 h and was maintained at peak levels until 72 h. As β-catenin is one of the known downstream targets activated by MUC1, we investigated expression levels of β-catenin. However, we did not observe any differences between SARS-

CoV-2 and mock infections. In addition to its role at the cell membrane, MUC1-C can function as an oncogene by translocating to the nucleus to activate transcription (13, 14). To determine if MUC1-C was imported to the nucleus after SARS-CoV-2 infection, we treated Calu-3 cells with Leptomycin B to inhibit nuclear export. We found that a small proportion of MUC1-C was present in nuclei after SARS-CoV-2 infection (Fig. 1B). In contrast, no MUC1-C signal was observed in the nuclei of uninfected control cells. These results suggest that MUC1-C signaling activity is substantially altered in Calu-3 cells after SARS-CoV-2 infection.

**MUC1-C expression is dependent on STAT3 activation in Calu-3 cells after SARS-CoV-2 infection**

We have previously reported that SARS-CoV-2 infection induces STAT3 phosphorylation in Calu-3 cells (21), and others have demonstrated that STAT3 influences MUC1 expression in lung cancer cells (22). Therefore, we investigated the effect of STAT3 inhibitors, including AG490, JAK inhibitor I, and S3I-201, on MUC1-C expression. In mock-infected Calu-3 cells, basal expression of MUC1-C was reduced by treatment with JAK inhibitor I but not by treatment with AG490 or S3I-201. Importantly, JAK inhibitor I also markedly reduced MUC1-C expression in SARS-CoV-2-infected Calu-3 cells (Fig. 1C). These result support that increased MUC1 expression after SARS-CoV-2 infection is dependent on JAK1/3 activation and subsequent STAT3 activation.

**MUC1-C contributes to cell survival in Calu-3 cells after SARS-CoV-2 infection**

To investigate the contribution of MUC1-C to cell survival and proliferation in SARS-CoV-2-infected Calu-3 cells, we inhibited the dimerization and functional activity of MUC1-C with the cell-penetrating peptide GO-201. GO-201 treatment increased the levels of cleaved PARP

and cleaved caspase-3, suggesting that GO-201 induces apoptosis after SARS-CoV-2-infection (Fig. 2A). Furthermore, the expression of c-Myc and cyclin D1 were reduced, implying decreased proliferation after GO-201 treatment in SARS-CoV-2-infected Calu-3 cells (Fig. 2A). These findings appear to be specific to inhibition of MUC1-C because we did not observe any evident effect of the control peptide CP-1 (2 μM). However, we observed that higher concentration of control peptide CP-1 (5 μM) has some GO-201-like effects suggesting non-specific inhibition of cell-permeable peptides at high concentration. Inhibition of MUC1 signaling did not prominently affect the expression of β-catenin in SARS-CoV-2-infected Calu-3 cells. Moreover, neither GO-201 nor CP-1 treatment had any effect in mock-infected Calu-3 cells (Fig. 2B). These results suggest that MUC1-C signaling contributes to cell survival and the maintenance of Calu-3 cells after infection with SARS-CoV-2.

**Effect of MUC1-C signaling on SARS-CoV-2 replication in Calu-3 cells**

To investigate the possible functions of MUC1-C in SARS-CoV-2 replication, we treated Calu-3 cells with GO-201 or CP-1 and measured virus replication by real-time PCR and plaque formation assays. We amplified *RdRP*, which is synthesized by SARS-CoV-2, to estimate the viral copy number. We found that treatment with GO-201 induced 10-fold higher copy numbers of viral RNAs compared to CP-1 treatment (Fig. 3A). Additionally, we assessed the viral titer by standard plaque formation assay; however, we did not find any significant differences in the number of plaques between treatment groups (Fig. 3B). Considering that GO-201 induces apoptosis of Calu-3 cells, it is likely that the higher viral copy numbers of the GO-201-treated samples resulted from the infection-incompetent virus RNAs released by the dead cells. Taken together, the effect of MUC1-C signaling on SARS-CoV-2 replication may be limited in Calu-3 cells.

## DISCUSSION

MUC1 is upregulated in lung cancer cells and is hyper-secreted in the airway mucus of COVID-19 patients, suggesting that it may play a role in both conditions (22). To understand the risk of lung cancer patients infected with SARS-CoV-2, we investigated the expression and function of MUC1-C in the lung cancer cell line Calu-3. Our results demonstrate that induction of MUC1-C in response to SARS-CoV-2 infection may contribute to the sustained growth of lung cancer cells instead of offering protection from SARS-CoV-2.

In normal epithelial cells, highly glycosylated MUC1-N interacts and forms heterodimers with the membrane subunit MUC1-C and functions as a barrier to pathogens (11, 23). However, in lung cancer cells, MUC1-N is released from the membrane by proteases, such as TNF-α converting enzyme and Matrix metalloproteinase-14 (24, 25). Furthermore, MUC1 expression is polarized to the luminal membrane in normal epithelial cells but is indiscriminately expressed throughout the membrane in lung cancer cells (26, 27). These observations suggest that the protective function of MUC1 is markedly reduced in lung cancer cells compared to normal epithelial cells. Therefore, we expect that malignant cells of lung cancer patients are more susceptible to SARS-CoV-2 infection (Fig. 4).

MUC1 is upregulated upon infection with respiratory viruses, such as respiratory syncytial virus and human metapneumovirus, in A549 epithelial cells (28, 29). Consistent with these reports, we found STAT3-dependent induction of MUC1 in Calu-3 cells after SARS-CoV-2 infection. Induction of MUC1 during SARS-CoV-2 infection may contribute to pathogen defense by reducing efficacious infection or as an immunomodulator in normal and cancerous epithelial cells. In contrast, some reports have suggested that high MUC1 expression may be problematic. For example, MUC1 and MUC5AC proteins are hyper-secreted in the airway mucus of COVID-19 patients and may contribute to dyspnea (22). Of note, these observations show induction of MUC1 in normal epithelial cells during SARS-

CoV-2 infection. We expect more complicated outcomes in lung cancer patients due to the diverse roles of MUC1-C as a pathogen barrier and an oncogene in cancer cells. MUC1-C interacts with other transcription factors, such as β-catenin, STAT3, and TP53 (13-15), and induces the expression of downstream genes, including MUC1, c-Myc, and cyclin D1 (Fig. 4). As we have previously demonstrated that SARS-CoV-2 infection induces STAT3 activation in Calu-3 cells (22), we hypothesize that MUC1-C induction and STAT3 activation create a positive feedback loop that further induces the expression of MUC1 in Calu-3 cells after SARS-CoV-2 infection. Moreover, we found that inhibition of MUC1-C signaling reduces the expression of proliferation-related proteins (c-Myc and cyclin D1) and enhances the expression of apoptosis-related proteins after SARS-CoV-2 infection in Calu-3 cells. However, the effect of MUC1 signaling on virus replication was not clear. These results suggest that induction of MUC1 expression during SARS-CoV-2 infection may trigger sustained growth of lung cancer cells instead of suppression of viral infection and replication.

There is evidence that COVID-19 poses a risk for lung cancer patients. A recent investigation of 102 COVID-19 patients with lung cancer demonstrated that COVID-19 was severe in lung cancer patients (62% hospitalized, 25% died), but the severity of COVID-19 was related more closely to patient-specific features, such as age, genetic variation, and smoking status, than cancer-specific characteristics (30). The conclusions that can be drawn from this study are limited by its relatively small scale and short time frame. Together with our present study, these findings indicate that extensive and long-term investigation is required to determine whether COVID-19 is an important risk factor for lung cancer patients. Nevertheless, our findings suggest that MUC1 expression is induced by SARS-CoV-2 and may contribute to the increased risk of lung cancer cells upon SARS-CoV-2. Importantly, we show that these effects can be targeted by inhibition of JAK-dependent STAT3 activation which may have important clinical implications for lung cancer patients who contract

COVID-19.

## MATERIALS AND METHODS

### Cell culture and virus

The human airway epithelial cell line, Calu-3, and African green monkey kidney cell line, Vero E6 cell, were obtained from the Korean Cell Line Bank. The cells were cultured in Dulbecco's modified Eagle's medium (DMEM, Thermo Fisher Scientific) containing 10% fetal bovine serum (FBS, Thermo Fisher Scientific), 25 mM HEPES, 100 U/ml penicillin, and 100 μg/ml streptomycin. The cells were incubated in atmospheric conditions of 95% air and 5% $CO_2$ at 37˚C. Severe acute respiratory syndrome coronavirus 2 (SARS-CoV-2, NCCP No. 43326) was provided by the National Culture Collection for Pathogens (Osong, Korea).

### Virus amplification and quantification

SARS-CoV-2 amplification and quantification was performed as described previously with minor modifications (21, 31, 32), and detailed information is provided in the Supplementary Material. SARS-CoV-2 amplification and cell culture procedures were performed in biosafety level 3 (BSL-3) conditions.

### Antibodies and Inhibitors

To detect the cytoplasmic tail of MUC1-C in cells by western blotting, we purchased a commercially available rabbit anti-MUC1-CT antibody from Abcam (Catalog No. ab109185). Antibodies to poly-ADP ribose polymerase (PARP, Catalog No. 9542S), cleaved caspase-3 (Catalog No. 9661S), c-Myc (Catalog No. 5605S), cyclin D1 (Catalog No. 2978S), and β-catenin (Catalog No. 8480S) were purchased from Cell Signaling Technology. Anti-β-actin (Catalog No. A5316) was obtained from Sigma-Aldrich. AG490, a JAK2 kinase inhibitor

(Catalog No. T3434), and S3I-201, a STAT3 dimerization inhibitor (Catalog No. SML0330), were purchased from Sigma-Aldrich. JAK inhibitor I (Catalog No. 420099), a potent ATP-competitive inhibitor of JAK1, JAK2, and JAK3, was purchased from Calbiochem. All inhibitors were dissolved in dimethyl sulfoxide (DMSO, Catalog No. 10378-73, Kanto Chemical). For inhibitor studies, cells were pretreated with 0.1% DMSO, 25 μM AG490, 20 μM S3I-201, or 1 μM JAK inhibitor I for 30 min. After pretreatment, cells were infected with SARS-CoV-2 at a MOI of 0.5 for 1 h and then cultured in DMEM containing 2% FBS for 48 h. GO-201, a MUC1-C inhibitor (d-RRRRRRRRR-CQCRRKNYGQLDIFP), and a control peptide (CP-1, d-RRRRRRRRR-AQARRKNYGQLDIFP) were synthesized by Anygen as described previously (33). Calu-3 cells were infected with SARS-CoV-2 at a MOI of 0.1. After viral infection, cells were treated with PBS or 2 μM of GO-201 or CP-1 and incubated for another 48 h.

**Western Blotting**

SARS-CoV-2-infected Calu-3 cells were lysed with cell lysis buffer (20 mM Tris-HCl, pH 8.0, 5 mM EDTA, 150 mM NaCl, 100 mM NaF, 2 mM $Na_3VO_4$, and 1% NP-40) and the cell lysates were run on SDS-PAGE and subsequently transferred onto a nitrocellulose membrane as described previously (22, 34), and detailed information is provided in the Supplementary Material.

**Confocal Images**

MUC1-C expression and localization was confirmed by confocal imaging as described previously (35, 36). Briefly, Calu-3 cells were cultured for 24 h on poly-L-lysine-coated glass cover slips in 12-well culture plates. The cells were washed with PBS and infected with SARS-CoV-2 at an MOI of 0.5. After 1 h, viral supernatants were removed and replaced with

2 ml of DMEM containing 2% FBS. The cells were incubated for 45 h at 37°C in a $CO_2$ incubator prior to treatment with PBS or Leptomycin B (LMB, Cell Signaling Technology, 20 nM), an inhibitor of chromosomal region maintenance 1 (CRM1) that is a nuclear export protein. After a 3 h treatment, the cells were prepared for immunofluorescent imaging as follows. Cells were fixed with 4% paraformaldehyde, permeabilized with 0.1% Triton X-100, blocked with 3% BSA, and incubated with rabbit anti-MUC1-CT antibody for 2 h at room temperature. After washing the cells with PBST (0.1% Triton X-100 in PBS) containing 1% BSA, the cells were incubated with Alexa Fluor 488-conjugated secondary antibody (Catalog No. A32790, Thermo Fisher Scientific) for 1 h at room temperature. Nuclei were stained with Hoechst 33258 (Thermo Fisher Scientific). Images were collected using a confocal laser scanning microscope system (CLSM, LSM 710, Carl Zeiss).

**Quantitative Real-time RT-PCR**

Viral particles were obtained from virus-infected cell culture supernatants, and quantification of the RNA-dependent RNA polymerase (*RdRP*) gene of SARS-CoV-2 was performed as described previously (21, 37), and detailed information is provided in the Supplementary Material.

**Statistical Analysis**

Results are shown as the mean ± standard deviation. The statistical significance of differences between two samples was evaluated using Student's t-test, and $P < 0.05$ was considered the threshold for statistical significance.

**ACKNOWLEDGMENTS**

This research was supported by grants from the National Research Foundation (NRF-2 016M3A9B6916708, NRF-2020M3A9I2107294) funded by the Ministry of Science and

ICT in the Republic of Korea.

## CONFLICTS OF INTEREST

The authors declare no conflict of interest.

## FIGURE LEGENDS

**Figure 1. MUC1-C expression in SARS-CoV-2-infected Calu-3 cells.** (A) Calu-3 cells were mock-infected as a control or infected with SARS-CoV-2 at a MOI of 0.5 for the indicated time periods. Cell lysates were prepared, and western blotting was performed with the indicated antibodies. β-actin was analyzed as a loading control. (B) Calu-3 cells were mock-infected or infected with SARS-CoV-2 at a MOI of 0.5. After 1 h of incubation, the viral medium was replaced with DMEM containing 2% FBS. After 45 h of incubation, the cells were treated with PBS or 20 nM Leptomycin B for 3 h. To evaluate localization of MUC1-C, cells were stained with anti-MUC1-CT (green) and Hoechst 33258 to visualize nuclei (blue). (C) Calu-3 cells were pretreated with 0.1% DMSO, 25 μM AG490, 1 μM JAK inhibitor I, or 20 μM S3I-201 for 30 min. The cells were washed with PBS, and then mock-infected or infected with SARS-CoV-2 in PBS at a MOI of 0.5. Cell lysates were prepared at 48 h and analyzed by western blotting.

**Figure 2. Inhibition of MUC1-C signaling enhances apoptotic protein expression in SARS-CoV-2-infected Calu-3 cells.** Calu-3 cells were mock-infected (A) or infected with SARS-CoV-2 at a MOI of 0.5 (B). After infection, the cells were treated with 2 μM of cell-penetrating peptides GO-201 or CP-1. Cell lysates were prepared 48 h after infection, and western blotting was performed with the indicated antibodies. β-actin was analyzed as a loading control.

**Figure 3. MUC1-C signaling modestly influences the replication of SARS-CoV-2.** Calu-3 cells (n = 3, 6-well plate) were infected with SARS-CoV-2 at a MOI of 0.1 prior to treatment with PBS, 2 μM GO-201, or 2 μM CP-1. Viral particles were collected from cell culture supernatants 48 h after infection, and virus quantification was performed by qRT-PCR analysis of the SARS-CoV-2 *RdRP* gene (A) and plaque formation assay (B). Significance was determined by comparison to the untreated control or CP-1 control. $^{**}P < 0.01$; ns, not significant.

**Figure 4. Modeling the influence of MUC1-C on cell survival in SARS-CoV-2-infected Calu-3 cells.** In lung cancer cells, MUC1-N domains are frequently released, which may weaken the protective function of MUC1 and sensitize cells to SARS-CoV-2 infection. Due to lack of interaction with MUC1-N, MUC1-C is internalized and interacts with transcription factors, such as β-catenin and phospho-STAT3. The MUC1 complex translocates to the nucleus and activates the transcription of several genes, such as MUC1, c-Myc, and cyclin D1, which contribute to the survival and proliferation of the infected cells. Several questions remain, including the mechanism of JAK1/3 activation after SARS-CoV-2 infection, and the putative function of viral proteins. Altogether, we suggest that SARS-CoV-2 infection may aggravate lung cancer via induction of MUC1 in a JAK/STAT3 activation-dependent manner.

## REFERENCES

1. Wu F, Zhao S, Yu B et al (2020) A new coronavirus associated with human respiratory disease in China. Nature 579, 265-269

2. Zhou P, Yang X, Wang X et al (2020) A pneumonia outbreak associated with a new coronavirus of probable bat origin. Nature 579, 270-273

315 3. Richardson S, Hirsch JS, Narasimhan M et al (2020) Presenting characteristics,
316 comorbidities, and outcomes among 5700 patients hospitalized with COVID-19 in the
317 New York city area. JAMA 323, 2052-2059

318 4. Yu J, Ouyang W, Chua MLK (2020) SARS-CoV-2 transmission in cancer patients of a
319 tertiary hospital in Wuhan. JAMA Oncol 6, 1108-1110

320 5. Sidaway P (2020) COVID-19 and cancer: What we know so far. Nat Rev Clin Oncol 17,
321 336

322 6. Bersanelli M (2020) Controversies about COVID-19 and anticancer treatment with
323 immune checkpoint inhibitors. Immunotherapy 12, 269-273

324 7. Siegel RL, Miller KD, Jemal A (2020) Cancer statistics, 2020. CA Cancer J Clin 70, 7-30

325 8. Russano M, Vincenzi B, Tonini G, Tonini G, Santini D (2020) Coronavirus disease 2019 or
326 lung cancer: What should we treat? J Thorac Oncol 15, e105-106

327 9. Zhang H, Huang Y, Xie C (2020) The treatment and outcome of a lung cancer patient
328 infected with severe acute respiratory syndrome coronavirus-2. J Thorac Oncol 15, e63-64

329 10. Hollingsworth MA, Swanson BJ (2004) Mucins in cancer: protection and control of the
330 cell surface. Nat Rev Cancer 4, 45-60

331 11. Levitin F, Stern O, Weiss M et al (2005) The MUC1 SEA module is a self-cleaving
332 domain. J Biol Chem 280, 33374-33386

333 12. Macao B, Johansson DG, Hansson GC, Härd T (2006) Autoproteolysis coupled to protein
334 folding in the SEA domain of the membrane-bound MUC1 mucin. Nat Struct Mol Biol 13,
335 71-76

336 13. Kufe DW (2009) Mucins in cancer: function, prognosis and therapy. Nat Rev Cancer 9,
337 874-885

338 14. Kufe DW (2013) MUC1-C oncoprotein as a target in breast cancer: activation of
339 signaling pathways and therapeutic approaches. Oncogene 32, 1073-1081

340 15. Ahmad R, Rajabi H, Kosugi M et al (2011) MUC1-C oncoprotein promotes STAT3
341 activation in an autoinductive regulatory loop. Sci Signal 4, ra9

16. Huang L, Chen D, Liu D, Yin L, Kharbanda S, Kufe D (2005) MUC1 oncoprotein blocks glycogen synthase kinase 3beta-mediated phosphorylation and degradation of beta-catenin. Cancer Res 65, 10413-10422

17. Awaya H, Takeshima Y, Yamasaki M, Inai K (2004) Expression of MUC1, MUC2, MUC5AC, and MUC6 in atypical adenomatous hyperplasia, bronchioloalveolar carcinoma, adenocarcinoma with mixed subtypes, and mucinous bronchioloalveolar carcinoma of the lung. Am J Clin Pathol 121, 644-653

18. Kaira K, Okumura T, Nakagawa K et al (2012) MUC1 expression in pulmonary metastatic tumors: a comparison of primary lung cancer. Pathol Oncol Res 18, 439-447

19. Xu M and Wang X (2017) Critical roles of mucin-1 in sensitivity of lung cancer cells to tumor necrosis factor-alpha and dexamethasone. Cell Biol Toxicol 33, 361-371

20. Lu W, Liu X, Wang T et al (2020) Elevated MUC1 and MUC5AC mucin protein levels in airway mucus of critical Ill COVID-19 patients. J Med Virol 10.1002/jmv.26406

21. Park BK, Kim D, Park S et al (2021) Differential signaling and virus production in Calu-3 cells and Vero cells upon SARS-CoV-infection. Biomol Ther (Seoul) doi.org/10.4062/biomolther.2020.226. in press

22. Gao J, McConnell MJ, Yu B et al (2009) MUC1 is a downstream target of STAT3 and regulates lung cancer cell survival and invasion. Int J Oncol 35, 337-345

23. Lindén SK, Sheng YH, Every AL et al (2009) MUC1 limits Helicobacter pylori infection both by steric hindrance and by acting as a releasable decoy. PLoS Pathog 5, e1000617

24. Thathiah A, Blobel CP, Carson DD (2003) Tumor necrosis factor-alpha converting enzyme/ADAM 17 mediates MUC1 shedding. J Biol Chem 278, 3386-3394

25. Thathiah A and Carson DD (2004) Mt1-Mmp mediates muc1 shedding independent of tace/adam17. Biochem J 382, 363-373

26. Nath S and Mukherjee P (2014) MUC1: a multifaceted oncoprotein with a key role in cancer progression. Trends Mol Med 20, 332-342

27. Kaira K, Nakagawa K, Ohde Y et al (2012) Depolarized MUC1 expression is closely associated with hypoxic markers and poor outcome in resected non–small cell lung cancer.

370 Int J Surg Pathol 20, 223-232

371 28. Li Y, Dinwiddie DL, Harrod KS, Jiang Y, Kim KC (2010) Anti-inflammatory effect of
372 MUC1 during respiratory syncytial virus infection of lung epithelial cells in vitro. Am J
373 Physiol Lung Cell Mol Physiol 298, L558-563

374 29. Baños-Lara Mdel R, Piao B, Guerrero-Plata A (2015) Differential mucin expression by
375 respiratory syncytial virus and human metapneumovirus infection in human epithelial cells.
376 Mediators Inflamm 2015, 347292

377 30. Luo J, Rizvi H, Preeshagul IR et al (2020) COVID-19 in patients with lung cancer. Ann
378 Oncol 31, 1386-1396

379 31. Kandeel M, Yamamoto M, Al-Taher A et al (2020) Small molecule inhibitors of Middle
380 East respiratory syndrome coronavirus fusion by targeting cavities on heptad repeat
381 trimers. Biomol Ther (Seoul) 28, 311-319

382 32. Park BK, Maharjan S, Lee SI et al (2019) Generation and characterization of a
383 monoclonal antibody against MERS-CoV targeting the spike protein using a synthetic
384 peptide epitope-CpG-DNA-liposome complex. BMB Rep 52, 397-402

385 33. Raina D, Ahmad R, Joshi MD et al (2009) Direct targeting of the mucin 1 oncoprotein
386 blocks survival and tumorigenicity of human breast carcinoma cells. Cancer Res 69, 5133-
387 5141

388 34. Shin MJ, Kim DW, Choi YJ et al (2020) PEP-1-GLRX1 protein exhibits anti-
389 inflammatory effects by inhibiting the activation of MAPK and NF-κB pathways in Raw
390 264.7 cells. BMB Rep 53, 106-111

391 35. Wu G, Kim D, Kim JN et al (2018) A mucin1 C-terminal subunit-directed monoclonal
392 antibody targets overexpressed mucin1 in breast cancer. Theranostics 8, 78-91

393 36. Wu G, Maharjan S, Kim D et al (2018) A novel monoclonal antibody targets mucin1 and
394 attenuates growth in pancreatic cancer model. Int J Mol Sci 19, 2004

395 37. Park BK, Kim J, Park S et al (2021) MERS-CoV and SARS-CoV-2 replication can be
396 inhibited by targeting the interaction between the viral spike protein and the nucleocapsid
397 protein. Theranostics 11, 3853-3867

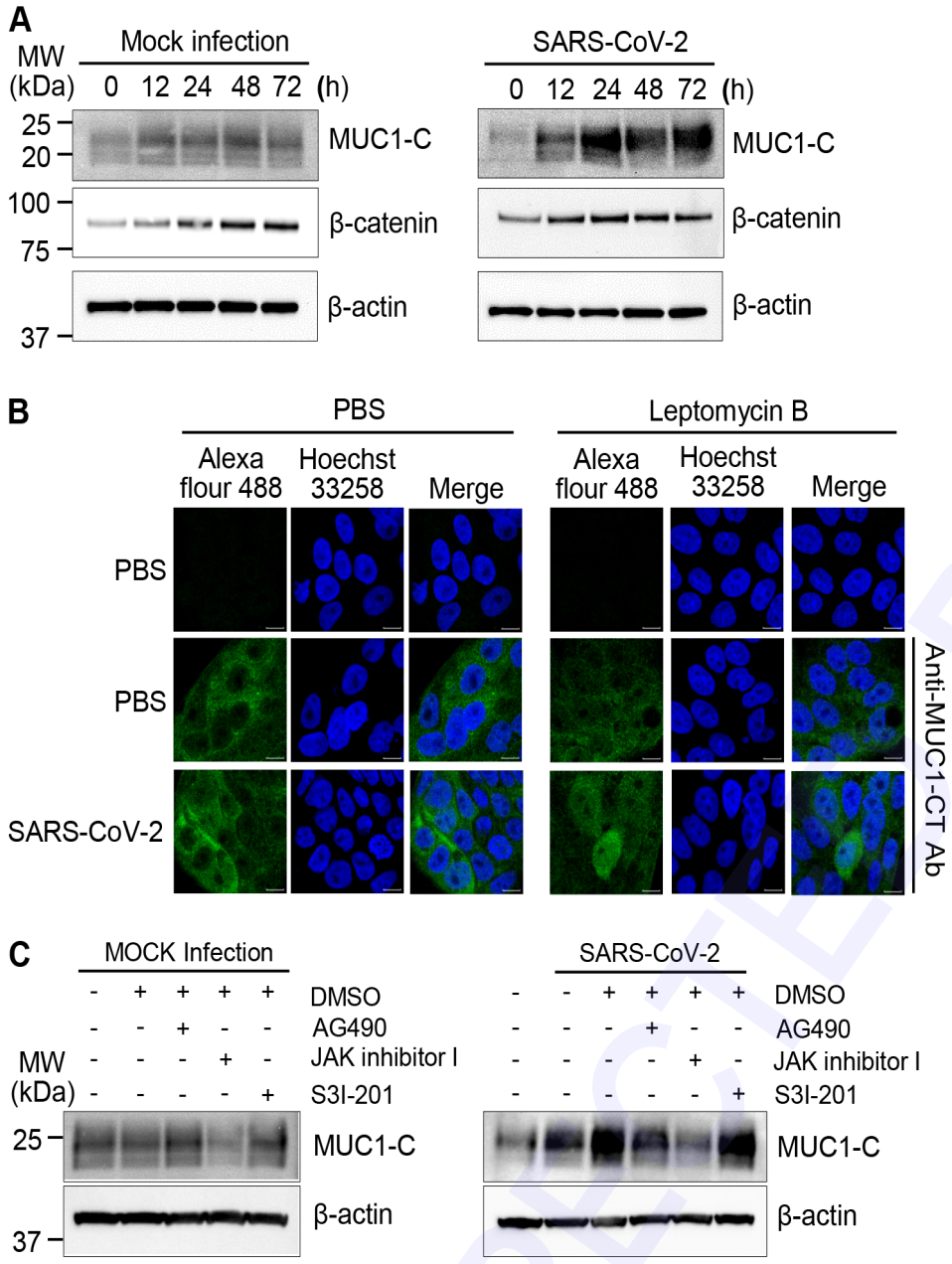


Fig. 1. Figure 1. MUC1-C expression in SARS-CoV-2-infected Calu-3 cells.

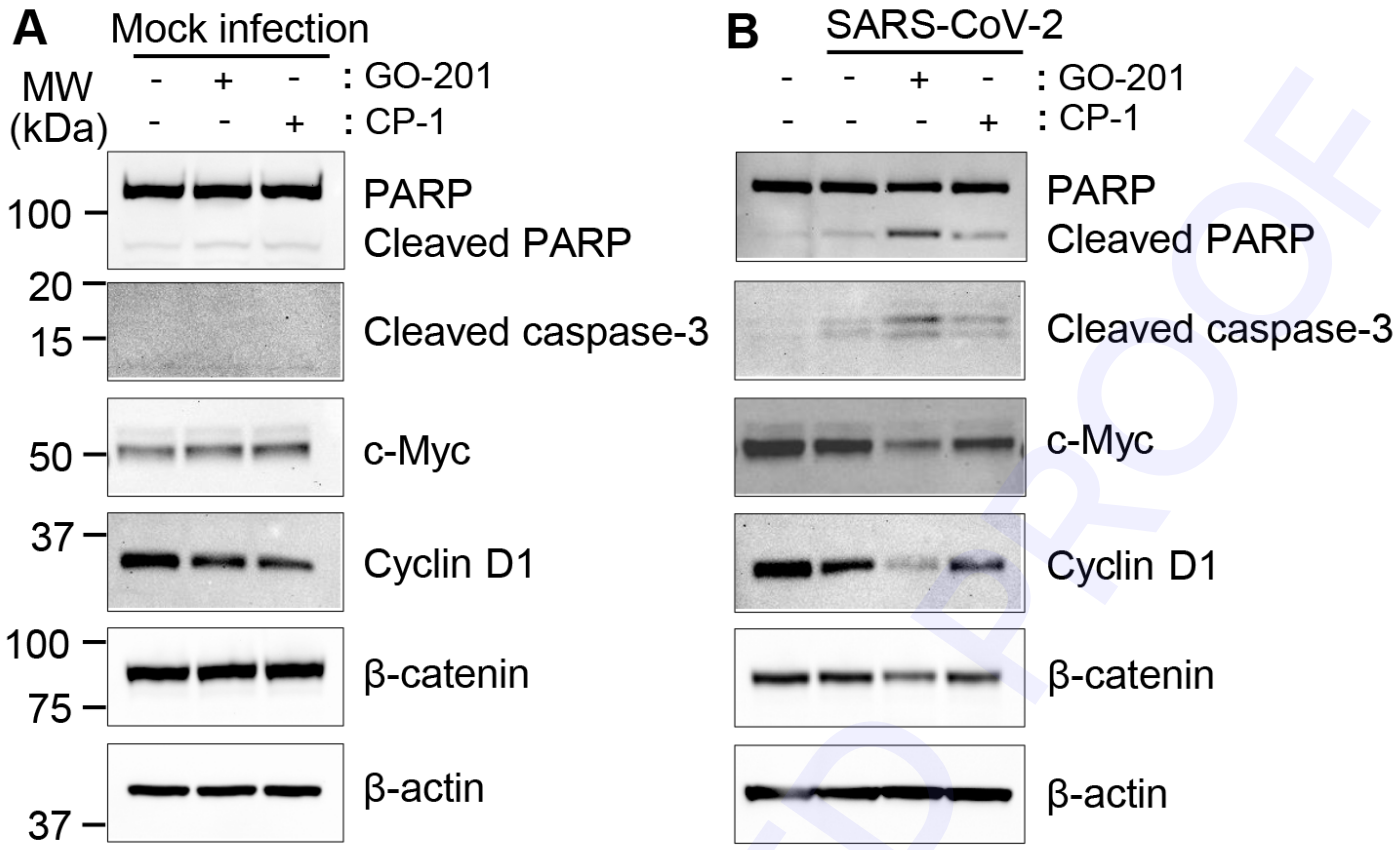


Fig. 2. Figure 2. Inhibition of MUC1-C signaling enhances apoptotic protein expression in SARS-CoV-2-infected Calu-3 cells.

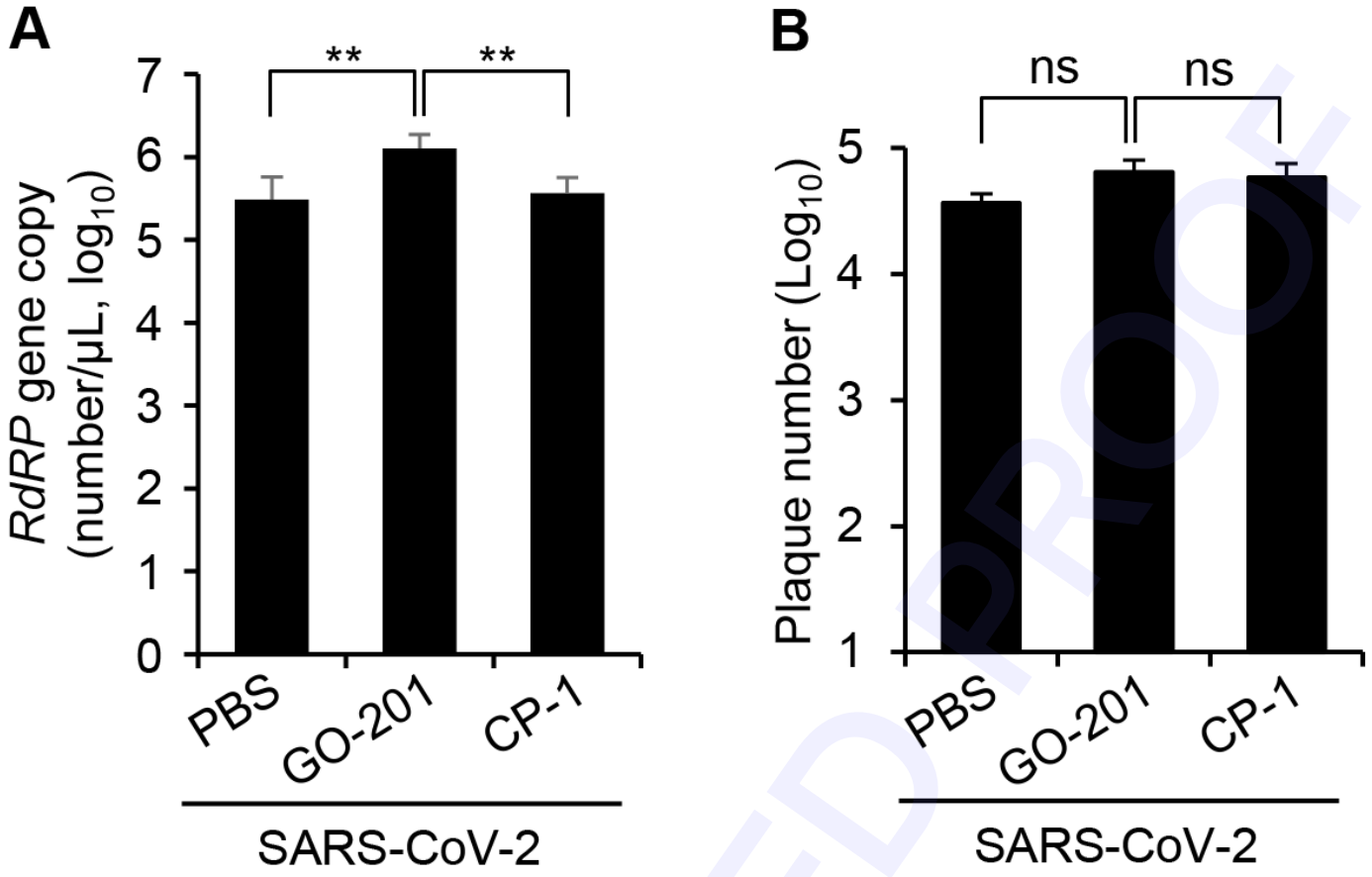


Fig. 3. Figure 3. MUC1-C signaling modestly influences the production of SARS-CoV-2.

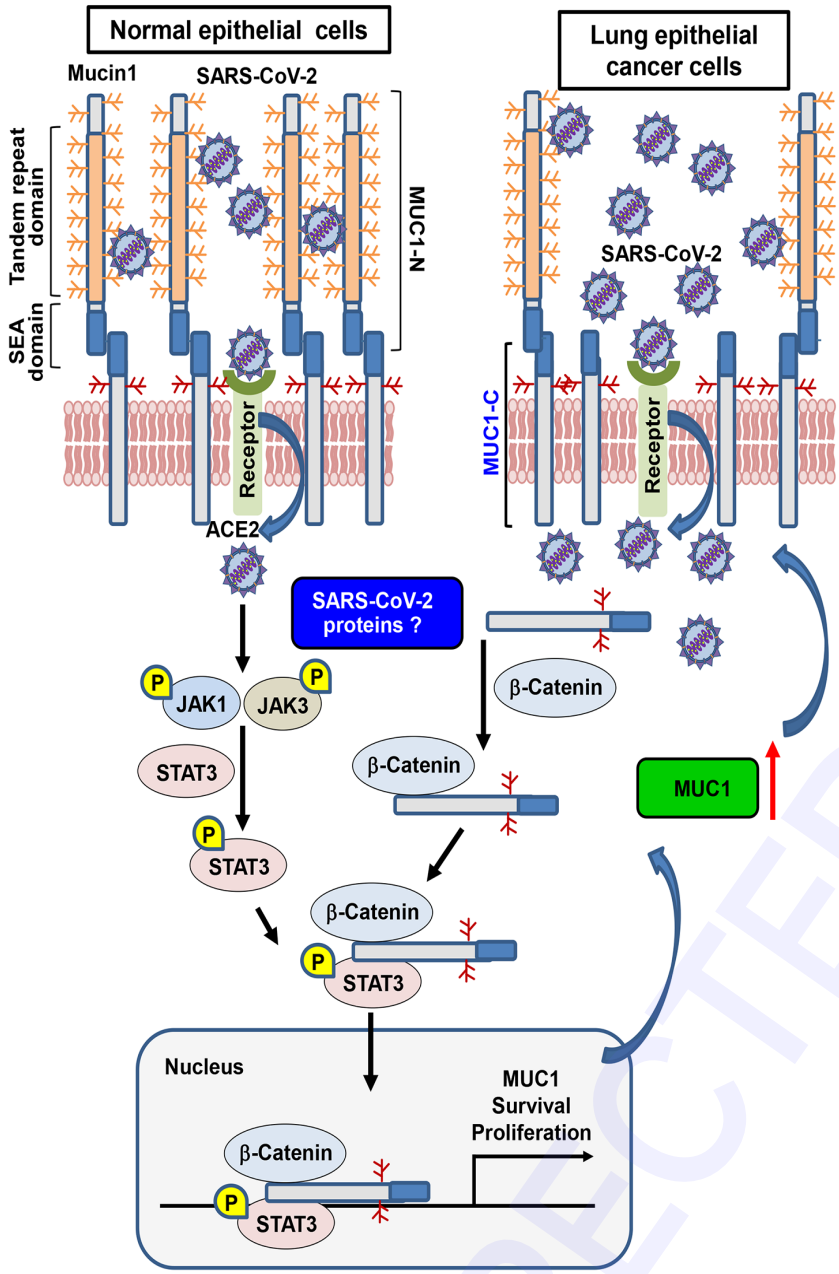


Fig. 4. Figure 4. Modeling the influence of MUC1-C on cell survival in SARS-CoV-2-infected Calu-3 cells.

**Manuscript Type: Article**

# MUC1-C influences cell survival in lung adenocarcinoma Calu-3 cells after SARS-CoV-2 infection

Dongbum Kim[1], Sony Maharjan[1], Jinsoo Kim[2], Sangkyu Park[3], Jeong-A Park[3], Byoung Kwon Park[1], Younghee Lee[3], Hyung-Joo Kwon[1,2]

[1]Institute of Medical Science, College of Medicine, Hallym University, Chuncheon 24252, Republic of Korea

[2]Department of Microbiology, College of Medicine, Hallym University, Chuncheon 24252, Republic of Korea

[3]Department of Biochemistry, College of Natural Sciences, Chungbuk National University, Cheongju 28644, Republic of Korea

## MATERIALS AND METHODS

### Virus amplification and quantification

Briefly, Vero E6 cells were plated at a density of $2 \times 10^5$ cells/well of a 6-well plate in DMEM containing 10% FBS and cultured at 37°C in a $CO_2$ incubator. After overnight culture, the cells were washed with PBS and treated with SARS-CoV-2 at an MOI of 0.01 in PBS. The cells were incubated with the virus for 1 h at 37°C in a $CO_2$ incubator. After incubation, the viral supernatant was replaced with 2 ml of DMEM containing 2% FBS. The cells were incubated at 37°C in a $CO_2$ incubator for 3 days. Finally, cell culture supernatants were harvested and centrifuged at 2,000 rpm for 10 min at 4°C to remove cell debris.

The amplified viral supernatants were quantified by plaque formation assay as follows. Vero E6 cells ($6 \times 10^5$ cells/well of a 6-well plate) were plated and cultured overnight at 37°C in a $CO_2$ incubator. The cells were then washed with PBS and infected with amplified SARS-CoV-2 after a 10-fold serial dilution. After 1 h of incubation at 37°C in a $CO_2$ incubator, viral supernatants were removed and replaced by DMEM/F12 (Thermo Fisher Scientific) containing 2% oxoid agar and N-*p*-Tosyl-L-phenylalanine chloromethyl ketone (TPCK, 1 μg/ml)-treated trypsin (Sigma-Aldrich). Plaques were allowed to develop for 72 h at 37°C. After 72 h, the plates were stained for 1 h with 0.1% crystal violet, and the number of plaques was counted. The quantified viruses ($5 \times 10^6$ pfu/ml) were aliquoted at 400 μl per Eppendorf tube and stored at –70°C.

### Western blotting

SARS-CoV-2-infected Calu-3 cells were lysed with cell lysis buffer (20 mM Tris-HCl, pH 8.0, 5 mM EDTA, 150 mM NaCl, 100 mM NaF, 2 mM $Na_3VO_4$, and 1% NP-40) and centrifuged at 14,000 rpm at 4°C for 20 min to prepare cell lysates. Equal amounts of protein were separated in

4–12% Bis-Tris gradient gels (Thermo Fisher Scientific) and transferred onto nitrocellulose membranes. The membranes were blocked with 3% BSA and incubated with primary antibody overnight at 4°C. After membrane incubation with a horseradish peroxidase-conjugated secondary antibody (Jackson ImmunoResearch), immunoreactive bands were developed with an enhanced chemiluminescence (ECL) reagent (Thermo Fisher Scientific).

**Quantitative Real-time RT-PCR**

Viral particles were obtained from virus-infected cell culture supernatants, and viral RNA was collected from the supernatants using the QIAamp Viral RNA Mini Kit (Catalog No. 52904, Qiagen) according to the manufacturer's instruction. cDNA was synthesized with the Reverse Transcription System kit (Catalog No. A3500, Promega). To quantify the transcription of the RNA-dependent RNA polymerase (*RdRP*) gene of SARS-CoV-2, we used the following primers: forward primer, 5′-GTGAAATGGTCATGTGTGGCGG-3'; reverse primer 5'-CAAATGTTAAAAACACTATTAGCATA-3'; and TaqMan® Probe 5'-FAM-CAGGTGGAACCTCATCAGGAGATGC-TAMRA-3'. Oligonucleotide sequences were synthesized by Genotech. Quantitative real-time RT-PCR (qRT-PCR) reactions contained 10 µL GoTaq® Probe qPCR Master Mix (catalog No. A6101, Promega) and 10 µL sample mixture including forward and reverse primer mix (125 nM each), 250 nM TaqMan Probe, and 1 µL cDNA. After initial denaturation at 95℃ for 5 min, 45 PCR cycles were performed at 95℃ for 15 sec and 60℃ for 1 min using Rotor-Gene Q (Qiagen). The *RdRP* copy number of each sample was calculated using a standard curve obtained from the cloned *RdRP* cDNA. Standard curve was drawn using a recombinant plasmid including *RdRP* cDNA. The *RdRP* cDNA was obtained using viral RNAs by RT-PCR using the following primer set: forward primer, 5′-

GTGAAATGGTCATGTGTGGCGG-3' and reverse primer, 5'-CAAATGTTAAAAACACTATTAGCATA-3'. The PCR product of the *RdRP* cDNA fragment was cloned into RBC T&A cloning vector (RBC, New Taipei City, Taiwan). Standard curve was generated using 10-fold serially diluted samples of the plasmid DNA, ranging from $1\times10^4$ to $1\times10^9$ copies/µl ($R^2 \geq 0.99$). The copy number was calculated using the following equation: DNA copy number = (DNA amount (ng) x 6.0221 x $10^{23}$ (molecules / mole)) / (DNA length (bp) x 660 (g/mole/bp) x 1 x $10^9$ (ng/g)).